

# TRANSPARENT LATTICE CHARACTERIZATION WITH GATED TURN-BY-TURN DATA OF DIAGNOSTIC BUNCH-TRAIN

Y. Li, W. Cheng\*, K. Ha and R. Rainer,

Brookhaven National Laboratory, Upton, New York 11973 USA

## Abstract

Methods of characterization of a storage ring's lattice have traditionally been intrusive to routine operations. More importantly, the lattice seen by particles can drift with the beam current due to collective effects. To circumvent this, we have developed a novel approach for dynamically characterizing a storage ring's lattice that is transparent to operations. Our approach adopts a dedicated filling pattern which has a short, separate Diagnostic Bunch-Train (DBT). Through the use of a bunch-by-bunch feedback system, the DBT can be selectively excited on-demand. Gated functionality of a beam position monitor system is capable of collecting turn-by-turn data of the DBT, from which the lattice can then be characterized after excitation. As the DBT comprises only about one percent of the total operational bunches, the effects of its excitation are negligible to users. This approach allows us to localize the distributed quadrupolar wake fields generated in the storage ring vacuum chamber during beam accumulation. While effectively transparent to operations, our approach enables us to dynamically control the beta-beat and phase-beat, and unobtrusively optimize performance of National Synchrotron Light Source-II accelerator during routine operations.

## INTRODUCTION

For high brightness synchrotron light sources, it is essential to mitigate lattice distortion to optimize performance during routine operations. At National Synchrotron Light Source-II (NSLS-II) [1], the deviation of the linear lattice has been observed but not quantitatively characterized during operations. Although there are several methods to characterize and correct the linear lattice during dedicated machine studies periods, they often interfere with stable beam conditions due to the magnitude of beam manipulation for lattice characterization. Common tools used for lattice characterization and/or correction include, but are not limited to: Linear Optics from Closed Orbit (LOCO) [2,3], TbT data of a short bunch-train excited by a short pulse excitation [4–9], or a long bunch-train excited by the bunch-by-bunch feedback system [10].

With modern advancements in BPM technology, storage ring lattices can be characterized with accurately aligned BPM turn-by-turn (TbT) data. To accomplish this, the beam is excited with a pulsed magnet, also known as a “pinger” magnet. At most light source facilities, however, the pulse width of a pinger wave usually lasts several micro-seconds, while the separation between two adjacent buckets is a few nanoseconds. Most of existing BPM systems are unable to

resolve the bunch-by-bunch signals. The TbT data that reveals the centroid motion of the long bunch-train is therefore highly decoherent after excitation [11–13]. To obtain clean TbT data with such a long pulse width, one would need to utilize a shorter bunch-train. Or one could utilize a well designed pulsed magnet with a wide flat top waveform [14].

Another method of exciting long bunch-trains with a bunch-by-bunch feedback system (BBFB) has been developed at Diamond light source [10]. The excitation amplitudes are small (significantly less than the beam size) but at high frequencies. Their method involves collecting the TbT data with dedicated signal processing, after excitation. To characterize the lattice during operations, however, requires excitation of the whole operational bunch train. To achieve comparable resolution as the pinger excitation technique, their method also requires continuous excitation of the whole operational bunch train. Hereby, our method introduces a more transparent technique for lattice characterization that utilizes a short diagnostic bunch-train (DBT) developed at NSLS-II [15]. The DBT is isolated from the main user bunch-train and transversely excited with the BBFB system [16]. The TbT data of the DBT is collected using the gated functionality of BPMs. As the DBT (10 bunches) comprises only about one percent of the total bunches, and the excitation amplitude is less than 1 millimeter, the effects on the global beam motion are negligible to users. Additionally, an “on-demand” triggering mode is utilized to minimize the disturbance on the circulating beam. With minimal beam disturbance, this approach is effectively transparent to the beamlines and can be applied at any time during operations without interfering with experiments, even ones requiring high sensitivity.

## SELECTIVE BUNCH EXCITATION AND GATED TBT DATA ACQUISITION

This section discusses the necessary requirements for lattice characterization by designing a technique which utilizes a dedicated filling pattern configuration, gated bunch-train excitation and data acquisition.

### *Diagnostic Bunch-Train (DBT)*

During routine operation, various collective instabilities are suppressed by the transverse BBFB system. High precision lattice characterization, however, requires beam excitation which the BBFB would normally prevent. To bypass this, a short DBT is filled and is separated from the main, long operational bunch-train (see Fig. 1). The BBFB can be configured to only stabilize the operational bunch train, and not the DBT. The separation between the DBT and the

\* W. Cheng and Y. Li contributed equally to this work

Content from this work may be used under the terms of the CC BY 3.0 licence (© 2018). Any distribution of this work must maintain attribution to the author(s), title of the work, publisher, and DOI.

main bunch-train(s) needs to be larger than 75 empty buckets (~ 150 ns) due to the  $\pm 10$  MHz bandwidth of the band pass filter. During normal operations, the BPM system needs to deliver both 10 Hz data for slow orbit monitoring and 10 kHz data for fast orbit feedback at all times. The 10Hz and 10 kHz data need to be ungated to include all the bunch signals and the radio frequency (RF) attenuation on the BPMs set to correspond to the beam current. To obtain clean TbT signals with good signal-to-noise ratio the charge of the DBT needs to be maintained at a level of  $\sim 1\%$  of the total charge of the operational bunches.

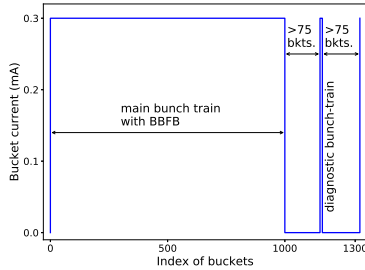


Figure 1: Bucket filling pattern with an extra DBT for transparent lattice characterization.

### Selective Bunch Excitation

The selective bunch excitation on the DBT is accomplished with the BBFB system. The digitizer of NSLS-II BBFB system has an integrated function that can excite any selected bunches [17]. It typically takes less than 2 ms for the betatron amplitude to reach about 1 mm (see Fig. 2). The excitation trigger is configured for an external, on-demand mode. The same trigger needs to be synchronized with the BPM gated data acquisition.

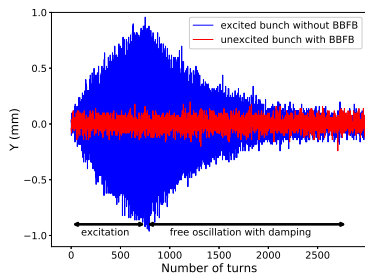


Figure 2: ADC signals (counts) from BPM buttons of an excited bunch (in blue) without BBFB suppression and an unexcited bunch (in red) with BBFB suppression. Excitation is performed through resonance driving for about 700 turns ( $\leq 2$  ms). Free betatron oscillation then decays through radiation damping.

There are several bunches in the DBT which need to be excited in phase. Therefore, the whole DBT is excited at the first harmonic of the betatron oscillation frequency. Measuring the TbT data of the different bunches in the DBT with the dedicated BBFB pick-up reveals centroid data that is consistent with our expected results (see Fig. 3).

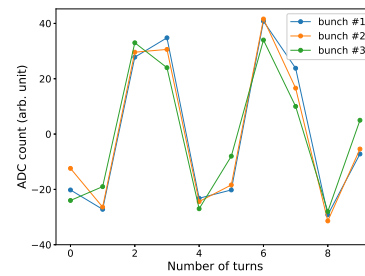


Figure 3: In-phase excitation of the DBT through resonance driving. Here the vertical ADC counts of 3 out of 10 bunches are shown. The signals are measured by the dedicated BPM used as the BBFB's pick-up, and its digitizer can distinguish different bunches in the train.

### Gated TbT Data Acquisition

The gated BPM data acquisition is accomplished through in-house BPM technology developed at NSLS-II. If the diagnostics bunches are separated by more than 150 ns, the digitizer is then capable of resolving them. The gated functionality of the BPMs has been implemented inside the field-programmable gate array. The schematic diagram of the gated signal processing is shown in Fig. 4. Two signal-processing channels with separated gates are provided. The delay and width of each gate can be adjusted independently so that signals from different bunch-trains can be selected and processed separately and simultaneously. One of the channels (Gate 2) can then be dedicated to lattice characterization. Expanding the number of channels could allow processing of multiple DBTs for possible future use.

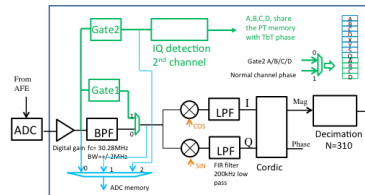


Figure 4: The schematic diagram of the gated signal processing. Two signal-processing channels with separated gates are provided. One of them (Gate 2) is dedicated to processing the DBT.

Under the filling pattern configuration seen previously in Fig. 1, TbT data is sampled at 117MHz with 310 samples per turn. The top of Fig. 5 illustrates the ADC raw data from one of the BPM buttons, labeled as "A". The signals from four buttons ("A-B-C-D") need to be overlapped and their cable delays must be well matched. The gate is then introduced (shown as the red boxes) and the signal processing only includes ADC data sampled from bunches inside the gap as illustrated at the bottom of Fig. 5. Fine timing alignment (8 ns steps) ensures all the BPMs around the ring process the signal from the same bunch(es).

For a short bunch-train, the gated TbT data has better resolution than the ungated TbT data [18], which can im-

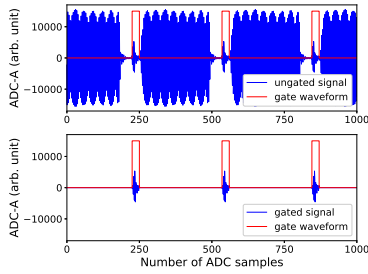


Figure 5: ADC signal of BPM button “A” with and without gated functionality. Ungated BPM signals are the sum of contributions from all buckets (top). After applying a gated waveform as illustrated by the red lines, the DBT signals can be filtered out and processed by the newly added channel (Gate 2) as seen in Fig. 4.

prove the lattice characterization precision. The improved resolution is noticeable in our measurements (see Fig. 6).

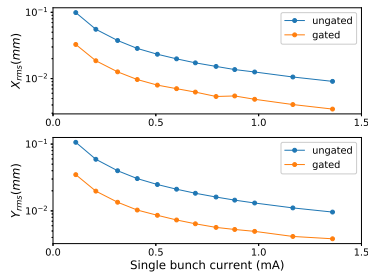


Figure 6: Comparison of the BPM resolutions for gated and ungated data. Gated BPM data resolution is measured  $\sim 3$  times better than the ungated data in both the horizontal and vertical planes.

Measured TbT data include BPM gain and roll errors, which require calibration before use. For each BPM, four pre-calibrated coefficients fitted from a measured orbit response matrix with LOCO [2] are implemented.

### Disturbance of User Beam

Beam disturbance during routine operations is something that all dedicated user facilities strive to minimize. As lattice characterization has traditionally required beam perturbation at levels that would affect users, particularly ones that require high sensitivity, it is important to note the impact that our technique has on the beam stability. To obtain the sufficient resolution for lattice characterization, the DBT amplitude is excited to a maximum of  $\sim 1$  mm in our case. The disturbance averaged over all bunches as seen by the ungated BPM signal, however, is only 1% or  $10 \mu\text{m}$  (see Fig. 7). The  $10 \mu\text{m}$  centroid oscillation can be damped within a few ms. It should also be noted that the negligible disturbance created by excitation of the DBT can be triggered on-demand, making this measurement transparent to users, even ones with highly sensitive equipment.

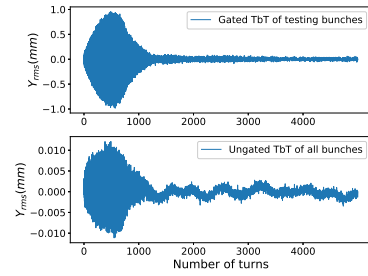


Figure 7: Comparison of the gated BPM TbT data of the DBT (top) and the ungated TbT data averaged over all filled buckets (bottom). Although the DBT amplitude reaches 1 mm for a few ms, the disturbance on the global beam stability is negligible. The ungated data of the combined bunch trains sees noise from either the power supplies or the RF cavities. Note that the two subplots’ vertical scales are different.

## LATTICE CHARACTERIZATION METHODS

This section briefly introduces the method used to characterize the linear lattice from TbT data at NSLS-II. There are other methods available as well, such as Principal component analysis (PCA) or model independent analysis (MIA) was proposed by Irwin and Wang [5, 6, 19], Independent Component Analysis (ICA) [7], which can be used for the same purpose, but are not covered here.

The approach of orthogonal decomposition [4] of beam TbT motion has been used. In the absence of damping and decoherence, and after eliminating the contribution from the closed orbit, the TbT betatron oscillation as seen by a BPM is

$$x_i = A\sqrt{\beta_x(s)} \cos[2\pi\nu_x \cdot i + \psi_x(s)] \quad (1)$$

Here,  $s$  is the location of the BPM,  $i \in [0, N - 1]$  is the index of consecutive turns, and  $x_i$  is the reading of the BPM at the  $i^{\text{th}}$  turn.  $A$  is a constant determined by the initial condition,  $\beta_x(s)$  and  $\psi_x(s)$  are the betatron envelope function and phase at the location of  $s$ , and  $\nu_x$  is the betatron tune per turn. Decomposing two orthogonal modes of the harmonic  $\omega_x = 2\pi\nu_x$  yields

$$C = \sum_{i=0}^{N-1} x_i \cos(2\pi\nu_x \cdot i), \quad S = \sum_{i=0}^{N-1} x_i \sin(2\pi\nu_x \cdot i) \quad (2)$$

The amplitude  $A\sqrt{\beta_x}$  and phase  $\psi_x$  can be obtained after some algebraic manipulation

$$A\sqrt{\beta_x} = \frac{2\sqrt{C^2 + S^2}}{N}, \quad \psi_x = -\tan^{-1}\left(\frac{S}{C}\right) \quad (3)$$

where the quadrant of the phase  $\psi_x$  can be determined by the signs of  $C$  and  $S$ . After determining the constant  $A$  by scaling the measured  $A^2\beta_x$  with the design  $\beta_{x,0}$ , a measured  $\beta_x$  can be obtained. In Eq. (3), the phase measurement is independent of the BPM gain calibration, which ensures an accurate characterization of the ring lattice.

Content from this work may be used under the terms of the CC BY 3.0 licence (© 2018). Any distribution of this work must maintain attribution to the author(s), title of the work, publisher, and DOI.

Once the lattice functions ( $\beta, \psi$ ) have been characterized, we can compare them with the design model. The distortion can be corrected iteratively with the linear response matrix between  $\beta, \psi$  and the focusing strength of the quadrupoles [7].

$$\begin{pmatrix} w_\beta \Delta\beta \\ w_\psi \Delta\psi \end{pmatrix} = \begin{pmatrix} w_\beta \mathbf{M}_\beta \\ w_\psi \mathbf{M}_\psi \end{pmatrix} \begin{pmatrix} \Delta K_1 \\ \Delta K_2 \\ \vdots \\ \Delta K_q \end{pmatrix}. \quad (4)$$

Here  $\Delta\beta = \beta_{meas.} - \beta_{model}$  are the  $\beta$ -beats as seen at the locations of BPMs,  $\Delta\psi = \psi_{meas.} - \psi_{model}$  are the phase-beats and  $w_{\beta, \psi}$  are the weights to balance the  $\beta$ -beat and phase-beat correction.  $\mathbf{M}_{\beta, \psi} = \frac{\partial(\beta, \psi)}{\partial K}$  are the response matrices of the beta and the phase depending on quadrupole strength.  $K_i = \frac{1}{B\rho} \left( \frac{\partial B_y}{\partial x} \right)_i, i = 1, 2, \dots$  is the  $i^{th}$  quadrupole's strength normalized with the beam rigidity  $B\rho$ .

## APPLICATIONS

In the past at NSLS-II, the lattice was optimized with ungated TbT data of a short bunch-train at a low current ( $N_{bunch} \leq 50, I_b \leq 2$  mA) excited by the pingers. During beam accumulation, tune drifting has been observed, corresponding to the beam current (Fig. 8). While injecting to higher operations currents, the injection efficiency occasionally drops off as well. Although the tune-drift can be monitored and corrected, it is typically not possible to localize the distribution of quadrupolar wake fields. To correct the tune under these circumstances requires blind selection of arbitrary quadrupoles to bring the tune back to the nominal value. Blind tune correction such as this often results in extra  $\beta$ -beat and phase-beat.

To measure the lattice drifting with the beam currents, a low charge DBT was injected into the ring. Gated BPM TbT data was then used to measure the lattice function and the correction algorithm from Eq. (4) was applied iteratively to reach a set of optimal magnet settings. For a such low beam current, the effect of the wake fields are negligible. The lattice is solely determined by the external magnetic fields and we refer to the measured lattice under these conditions as the reference lattice. A long bunch-train with 1,000 bunches, which is used for operations, was then filled. Instead of filling a Camshaft bunch as has become our standard operating procedure, however, we filled a 10-bunch train in place of the Camshaft bunch. The total charge inside the diagnostic train was maintained at a level of about 1% of the total charge during beam accumulation. At different beam currents, the DBT was selectively excited and its gated TbT data was collected by all 180 BPMs around the ring for lattice characterization. When the stored beam was above  $\sim 50$  mA, the beam became unstable. It was then necessary to have the BBFB system act on the main operational bunch train to suppress its instabilities.

From the gated BPM TbT data at different currents, we found the lattice was distorted gradually by the wake fields.

Tune-shift,  $\beta$  and  $\psi$ -beat relative to the stored beam currents are illustrated in Fig. 8 and 9. The tune dependence on the beam current has contributions from both dipolar and quadrupolar wake fields. Dipolar fields shift tunes in both planes negative, while quadrupolar fields shift tunes in both planes in opposite directions. From Fig. 8 we see that the horizontal and the vertical tunes drift in opposite directions, and the vertical tune shifts faster than the horizontal one. Based on this, it seems most likely that the lattice distortion is mainly due to the quadrupolar wakes of the long-range wake fields of the non-circular vacuum chambers with finite resistivity [20].

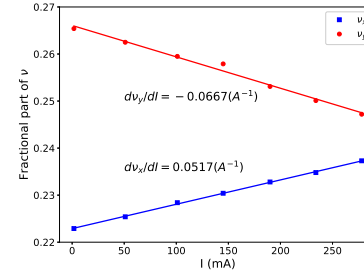


Figure 8: Tune-shifts with stored beam current.

The phase information of betatron oscillation can be measured more precisely than the envelope function  $\beta$ , therefore our lattice corrections rely heavily on the phase measurement in Eq. (4).

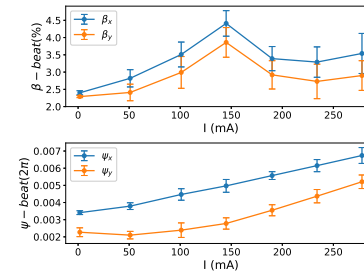


Figure 9:  $\beta$ -beat (top) and phase-beat (bottom) in relation to stored beam currents.

Based on the measured  $\beta$  and  $\psi$ -beats we can use Eq. (4) to locate the quadrupolar wake fields by putting numerous virtual quadrupoles around the ring. In Fig. 10, the variation of the vertical phase advance as a function of beam current is shown around the location of a 7 m long damping wiggler, which has a flat chamber.

Tune-drifts that correspond to beam current have been observed previously in several other high-energy storage rings and therefore are well understood [20–22]. The distributed wake fields were localized at other machines during dedicated beam study time [23, 24]. With the advent of our method, it is now possible to measure not only the incoherent tune-drifts, but also the distributed  $\beta$ -beat and phase-beat around the storage ring during user operation. A systematic correction strategy can therefore be implemented to mitigate distortion of the linear lattice.

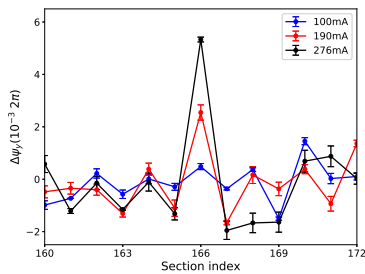


Figure 10: Variation of the vertical phase advance as a function of beam current around the location of a 7 m long damping wiggler (section 166), which has a flat chamber.

The dynamic aperture of modern storage rings' is highly sensitive to the phase advance among the sextupoles. At NSLS-II, 10-15% decrease in injection efficiency was frequently observed at the current nominal operating current (275-300 mA). To understand that, a simulation code, EL-EGANT [25], was used to simulate the distorted lattice dynamic aperture. The simulation involved adding the corresponding quadrupole strength adjustments on top of the external quadrupole settings directly. The dynamic aperture was found to decrease gradually with increasing beam current if no linear lattice correction was implemented (see Fig. 11). Injection efficiency can sometimes be restored more or less by blindly moving the horizontal and vertical tunes back to their nominal values. The lattice distortion, however, cannot be restored in this fashion. If the lattice continues to become more distorted by repeatedly adjusting the tunes blindly, it could result in a reduction of the local energy acceptance (LMA) as well as the Touschek lifetime.

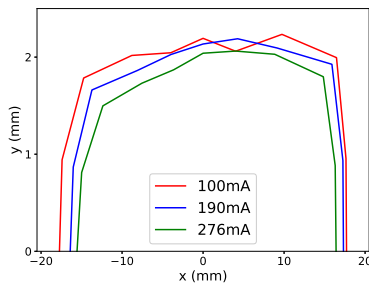


Figure 11: Dynamic aperture reduction at different stored beam currents without linear lattice correction at NSLS-II. In addition to the quadrupole nominal settings, localized quadrupolar wake fields are introduced in the lattice. The systematic and random multipole errors, closed orbit distortion and linear coupling are included in the simulations. Each dynamic aperture is obtained, accounting for random multipole error distributions in specific magnets, and averaged over 50 random seeds.

After accumulating  $\sim 275$  mA in NSLS-II storage ring, the lattice distortion was mitigated with 300 independently powered quadrupoles. The  $\beta$ -beat and phase-beat after correction was worse than at 2 mA, but was significantly improved compared to the uncorrected lattice. Lattice distortion

cannot be completely eliminated, owing to the quadrupolar wake fields generated at locations of noncircular vacuum chambers, such as dipoles chambers. While the quadrupoles used for lattice compensation are not located at the exact points of measurement, the lattice distortion can only be mitigated to a certain extent. Presently, NSLS-II operates at a stored beam current of 300 mA. Even at such a current the lattice distortion due to the quadrupolar wake fields is tolerable after a blind tune correction. The goal at NSLS-II is to eventually operate at Top-Off current of 500 mA. At this elevated current, lattice distortion can be expected to be greater and may not be as tolerable to blind tune corrections. It would therefore be prudent to implement a real-time lattice monitoring and correction program by scaling the wake fields with the beam current linearly.

## SUMMARY

As a premiere 3<sup>rd</sup> generation synchrotron light source, it is therefore paramount that performance of the accelerator is optimal. A key component of optimizing performance is minimizing linear lattice distortion. Traditional methods of lattice characterization have been intrusive during routine operations. We offer an improved, transparent approach. Our method applies selective gated transverse excitation and data acquisition of a small DBT. It overcomes several difficulties faced by traditional methods; common ones being interruption or disturbance of beamline experiments, or characterizing and correcting distortion from dynamic sources such as wake fields generated in vacuum chambers. Although the BPM system electronics at NSLS-II can be configured to resolve the signals of two well-separated bunch-trains, it will be necessary to develop a high resolution bunch-by-bunch BPM electronics system [26] to further improve diagnostics capabilities and therefore optimize machine performance.

## ACKNOWLEDGMENTS

We would like to thank our NSLS-II colleagues for supporting this study. This work was supported by Department of Energy Contract No. DE-SC0012704.

## REFERENCES

- [1] BNL, <https://www.bnl.gov/nsls2/project/PDR/>
- [2] J. Safranek, "Experimental determination of storage ring optics using orbit response measurements", *Nucl.Instrum.Meth.*, A 388, 1997, p.27-36.
- [3] X. Huang, J. Safranek and G. Portmann, "LOCO with constraints and improved fitting technique", *ICFA Beam Dyn. Newslett.*, Vol. 44, 2007, p. 60-69.
- [4] P. Castro-Garcia, "Luminosity and beta function measurement at the electron-positron collider ring LEP", CERN school, 1996, <http://www-spines.fnl.gov/spines/find/books/www?cl=CERN-SL-96-070-BI>
- [5] J. Irwin, C.X. Wang, Y.T. Yan, K.L.F. Bane, Y. Cai, F.J. Decker, M.G. Minty, G.V. Stupakov and F. Zimmermann, "Model-independent beam dynamics analysis", *Phys.*

- Content from this work may be used under the terms of the CC BY 3.0 licence (© 2018). Any distribution of this work must maintain attribution to the author(s), title of the work, publisher, and DOI.
- Rev. Lett.*, Vol. 82, 1999, p. 1684-1687. doi:10.1103/PhysRevLett.82.1684
- [6] C.X. Wang, "Model independent analysis of beam centroid dynamics in accelerators", at school at Stanford U., Phys. Dept., 1999.
- [7] X. Huang, S. Lee, E. Prebys, and R. Tomlin, "Application of independent component analysis to Fermilab Booster", *Phys. Rev. ST Accel. Beams*, Vol. 8, 2005, p. 064001. doi: 10.1103/PhysRevSTAB.8.064001
- [8] R. Tomás, M. Aiba, A. Franchi and U. Iriso, "Review of linear optics measurement and correction for charged particle accelerators", *Phys. Rev. Accel. Beams*, Vol. 20, 5, 2017, p. 054801, doi:10.1103/PhysRevAccelBeams.20.054801
- [9] A. Franchi, "Error analysis of linear optics measurements via turn-by-turn beam position data in circular accelerators", arXiv:1603.00281, 2016
- [10] G. Rehm, M.G. Abbott, A.F.D. Morgan, J. Rowland and I. Uzun, "Measurement of Lattice Parameters Without Visible Disturbance to User Beam at Diamond Light Source", BIW, 2010.
- [11] R.E. Meller, A.W. Chao, J.M. Peterson, S.G. Peggs and M. Furman, "Decoherence of Kicked Beams", SSC-N-360, 1987.
- [12] S.Y. Lee, "Decoherence of the Kicked Beams II", SSC-N-749, 1991.
- [13] I. Karpov, V. Kornilov and O. Boine-Frankenheim, "Early transverse decoherence of bunches with space charge", *Phys. Rev. Accel. Beams*, Vol. 19, 12, 2016, p. 124201. doi:10.1103/PhysRevAccelBeams.19.124201
- [14] P. Lebasque, R. Ben El Fekih, M. Bol, J.P. Lavieville, A. Loulergue and D. Muller, "Improvement on Pulsed Magnetic Systems at SOLEIL", Particle accelerator. Proceedings, 11th European Conference, EPAC 2008, Genoa, Italy, June 23-27, 2008, WEPC081.
- [15] W. Cheng, Y. Li and K. Ha, "Techniques for transparent lattice measurement and correction", *J. Phys. Conf. Ser.*, Vol. 874, 1, 2017, p. 012082, doi:10.1088/1742-6596/874/1/012082
- [16] W. Cheng, B. Bacha, D. Teytelman, Y. Hu, H. Xu and O. Singh, "Commissioning of Bunch-by-bunch Feedback System for NSLS2 Storage Ring", Proceeding of IBIC2014, Monterey, CA, USA, 2014, p. 707.
- [17] Dimtel Inc., <http://www.dimtel.com>
- [18] B. Podobodov, W. Cheng, K. Ha, Y. Hidaka, J. Mead, O. Singh and K. Vetter, "Single Micron Single-Bunch Turn-by-Turn BPM Resolution Achieved at NSLS-II", Proceedings of 7th International Particle Accelerator Conference (IPAC 2016, Busan, Korea, May 8-13, 2016, WEOBB01, doi:10.18429/JACoW-IPAC2016-WEOBB01
- [19] C.X. Wang, V. Sajaev and C.Y. Yao, "Phase advance and beta function measurements using model-independent analysis", *Phys. Rev. ST Accel. Beams*, Vol. 6, 2003, p. 104001, doi: 10.1103/PhysRevSTAB.6.104001
- [20] A. Chao, S. Heifets and B. Zotter, "Tune shifts of bunch trains due to resistive vacuum chambers without circular symmetry", *Phys. Rev. ST Accel. Beams*, Vol. 5, 2002, p. 111001, doi: 10.1103/PhysRevSTAB.5.111001
- [21] P. Brunelle, R. Nagaoka and R. Sreedharan, "Measurement and analysis of the impact of transverse incoherent wakefields in a light source storage ring", *Phys. Rev. Accel. Beams*, Vol. 19, 4, 2016, p. 044401, doi:10.1103/PhysRevAccelBeams.19.044401
- [22] A. Blednykh, G. Bassi, Y. Hidaka, V. Smaluk and G. Stupakov, "Low-frequency quadrupole impedance of undulators and wigglers", *Phys. Rev. Accel. Beams*, Vol. 19, 10, 2016, p. 104401, doi:10.1103/PhysRevAccelBeams.19.104401
- [23] D. Brandt, P. Castro, K. Cornelis, A. Hofmann, G. Morpurgo, G.L. Sabbi, J. Wenninger and B. Zotter, "Measurement of impedance distributions and instability thresholds in LEP", Proceedings of 16th Particle Accelerator Conference and International Conference on High-Energy Accelerators, HEACC 1995: Dallas, USA, May 1-5, 1995, p. 570-572.
- [24] V. Sajaev, "Transverse impedance distribution measurements using the response matrix fit method at APS", *ICFA Beam Dyn. Newslett.*, Vol. 44, 2007, p. 101-109.
- [25] M. Borland, "elegant: A Flexible SDDS-Compliant Code for Accelerator Simulation", *Advanced Photon Source LS-287*, 2000.
- [26] J. Shanks, D. Rubin and D. Sagan, "Low-emittance tuning at the Cornell Electron Storage Ring Test Accelerator", *Phys. Rev. ST Accel. Beams*, Vol. 17, 4, 2014, p. 044003, doi: 10.1103/PhysRevSTAB.17.044003